

## Non-free-electron momentum- and thickness-dependent evolution of quantum well states in the Cu/Co/Cu(001) system

Eli Rotenberg,<sup>1</sup> Y. Z. Wu,<sup>2,3</sup> J. M. An,<sup>1</sup> M. A. Van Hove,<sup>1,3,5</sup> A. Canning,<sup>4</sup> L. W. Wang,<sup>4</sup> and Z. Q. Qiu<sup>2,3</sup>

<sup>1</sup>Advanced Light Source, Lawrence Berkeley National Laboratory, Berkeley, California 94720, USA

<sup>2</sup>Department of Physics, University of California, Berkeley, California 94720, USA

<sup>3</sup>Materials Sciences Division, Lawrence Berkeley National Laboratory, Berkeley, California 94720, USA

<sup>4</sup>Computational Research Division, Lawrence Berkeley National Laboratory, Berkeley, California 94720, USA

<sup>5</sup>Department of Physics, University of California, Davis, California 95616, USA

(Received 11 May 2005; revised manuscript received 27 December 2005; published 21 February 2006)

We present systematic  $k_{\parallel}$ -dependent measurements of the Fermi surface and underlying band structure of quantum well states in Cu/Co/Cu(001). Compared to bands from normal emission, we find a complicated evolution of “split” quantum well states as a function of the thicknesses of both the copper overlayer and the cobalt barrier layer. Self-consistent calculations show that the penetration of the quantum well states into the cobalt barrier layer is significant and leads to the observed very non-free-electron behavior of these states.

DOI: [10.1103/PhysRevB.73.075426](https://doi.org/10.1103/PhysRevB.73.075426)

PACS number(s): 73.21.Fg, 79.60.-i, 71.18.+y

Quantum well (QW) states in magnetic transition metal multilayers are important both fundamentally and from a practical point of view. The most interesting technological prospect is that the magnetic properties of devices could be controlled by engineering the wave functions within layered structures through control of growth, geometry and composition. In order to achieve this level of control, a detailed understanding (both experimentally and theoretically) of the electronic and magnetic properties of multilayer devices is important.

QW states are usually described within a free-electron-like model modified by phase accumulation upon reflection at the interfaces,<sup>1</sup> which leads to simple parabolic bands. The phase at the substrate/QW interface is sensitive to the band structure of the substrate, especially near edges of the surface-projected band structure. This leads to an influence of the substrate on the QW states which can be probed by momentum- ( $\mathbf{k}$ -) resolved photoemission<sup>2</sup> or inverse photoemission<sup>3</sup> measurements. In these studies it was shown that the essential quantum numbers of the phase accumulation model (PAM) are not altered by the substrate interaction; only the parabolic form of the bands is modified, tending towards a flattening or kink of the QW bands as they cross substrate band edges. Recently, more complicated perturbations of the QW bands have been observed which were attributed to many-body interactions.<sup>4</sup>

In this paper, we show that the substrate can extend its influence beyond perturbation of the bands determined by simple phase accumulation models. In other words, the effect of the substrate is not just to change the interface reflection phase in the PAM so that the simple PAM breaks down. The reason is that when  $k_{\parallel} \neq 0$ , the Cu *sp* band interacts strongly with the Co minority *d* band. As a result, it is not enough to consider the Cu layer alone for determining the QW electronic structures; instead the substrate and overlayer metals must be treated as a unified system. We report detailed momentum-dependent measurements of the electronic properties of the Cu/Co/Cu(001) system, in which we find that while the simple PAM description suffices to describe the bands near normal emission, the band structure at in-plane

momentum  $k_{\parallel} \neq 0$  is more complicated. Furthermore, these bands have a complicated evolution as a function of both copper overlayer as well as cobalt barrier layer thickness. Self-consistent theoretical interpretation of the data is complicated by the large number of atoms needed for simulation (order of 30 atoms per unit cell); nevertheless, preliminary calculations are presented which show that the QW wave function penetration into the cobalt barrier layer is responsible for the observed behavior.

Experiments were performed on samples grown *in situ* at Beamline 7.0.1.2 (Electronic Structure Factory) of the Advanced Light Source and analyzed with an imaging-type angle-resolving hemispherical spectrometer (Gammadata SES-100). The samples were grown pseudomorphically (i.e., maintaining the lateral substrate periodicity throughout the deposited films) by room temperature deposition of Cu and Co onto Cu(001) crystals cleaned by Ar ion sputtering followed by annealing. The Cu thickness can be determined precisely by counting the discrete QW states observed at normal emission, while the Co barrier layer thickness is estimated by monitoring growth with a quartz crystal oscillator. The absolute Co thickness uncertainty is about  $\pm 1$  monolayer (ML) while the relative thicknesses are accurate to within about 10%. The dependence of the QW states on layer thicknesses ( $d_{\text{Cu}}, d_{\text{Co}}$ ) was systematically probed by growing wedge-profiled samples in which one thickness was varied while the other was held fixed; samples were probed with a 50  $\mu\text{m}$  photon spot. The angular-dependent photoemission patterns at photon energy 83 eV were measured while rotating the samples on a goniometer capable of two orthogonal polar rotations. Conversion from emission angle to momentum was through simple trigonometric transformation. The combined energy resolution (photon+electron) was better than 50 meV.

Figure 1(a) shows the angular distribution of states at the Fermi energy ( $E_F$ ) for a wide range of momenta  $\mathbf{k}_{\parallel} = (k_{[110]}, k_{[\bar{1}10]})$  for a 30 ML Cu film on 10 ML of Co on Cu(001) substrate. Except for some deviation near momentum  $k = 0.8 \text{ \AA}^{-1}$  (expected because of the influence of the “neck” region of the bulk Fermi surface) the data show an

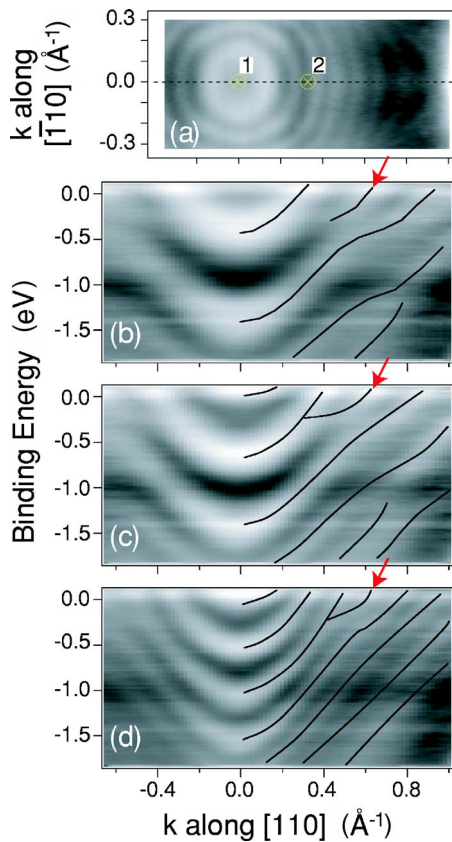


FIG. 1. (Color online) Fermi surface and band structure for Cu/Co/Cu(001) layered structures with variable  $d_{\text{Cu}}$  and fixed  $d_{\text{Co}}=10$  ML (lighter gray means stronger photoyield). (a) Fermi surface for  $d_{\text{Cu}}=30$  ML, (b–d) band maps along the dashed line in (a) for  $d_{\text{Cu}}=9.6$ , 12.8, and 22.4 ML, resp. The lines are guides for the eye.

array of nearly circular contours. In a simple nearly free-electron picture with plane-wave-like wave functions, these states disperse parabolically inward in momentum towards  $\mathbf{k}_{\parallel}=0$  as the binding energy is increased. What is surprising is that for all thicknesses  $d_{\text{Cu}}$  measured, at least one of these contours has entirely different dispersion character and cannot be explained within this simple free-electron model. This is illustrated by band structure measurements for three different QW thicknesses  $d_{\text{Cu}}$  in Figs. 1(b)–1(d). These figures are comprised of individual electron distribution curves as a function of  $k_{[110]}$ . For each thickness there appears to be an “extra” band (indicated by arrows) appearing around 0.4 eV binding energy and dispersing outwards toward the Fermi energy. While it is tempting to connect this extra band to one or another adjacent band, at some thicknesses [such as Fig. 1(b)] it is difficult to do that. The anomalous bands in Fig. 1 are located near  $k_{[110]}=0.5 \text{ \AA}^{-1}$  regardless of Cu film thickness, suggesting that they might be related to some features of the underlying Co band structure which is independent of the QW thickness.

Figure 2(a) shows the Cu thickness dependence of the electron distribution curves at normal emission [point 1 of Fig. 1(a)]. These data consist of discrete peaks joined by a diffuse background (typical for Cu/Co structures grown at

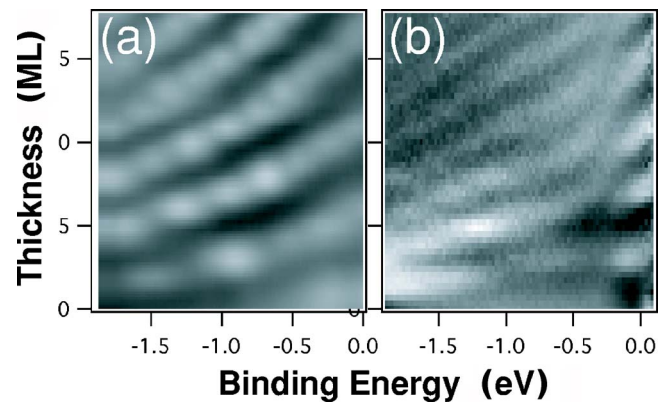


FIG. 2. (Color online) Energy distribution curves as a function of Cu thickness  $d_{\text{Cu}}$  for (a) normal emission [point 1 of Fig. 1(a)] and (b) off-normal [point 2 of Fig. 1(a)].

room temperature) whose intensity is a function of the sample film quality. The position of the discrete peaks has been discussed theoretically within simple empirical<sup>5</sup> and elaborate self-consistent<sup>6</sup> schemes and can be approximated well using simple plane-wave states within a phase accumulation model. Figure 2(b) shows a similar data set collected for off-normal emission [point 2 of Fig. 1(a)]. Contrary to normal emission, these data show that the off-normal states do not evolve uniformly but appear to display anti-crossing behavior, especially around  $-0.4$  eV binding energy. The behavior is reminiscent of the normal emission data for double QW structures, in which the evolution of states as a function of outer QW thickness has anti crossings at the discrete energy levels of a fixed inner QW [see Ref. 7, esp. Fig. 2(c)]. This suggests the interaction in the present case between QW states and states in the underlying Co substrate, which are likely to be a more complicated interaction than in the simple example of Ref. 7.

The results of Figs. 1 and 2 implicate the underlying Co states in the modifications of the QW band structure. Therefore we now consider the dependence of the QW states on the Co barrier layer thickness ( $d_{\text{Co}}=3\text{--}8$  ML) at constant Cu QW thickness ( $d_{\text{Cu}}=19$  ML); results are shown in Fig. 3. At all Co thicknesses there appears a similar split-off band (indicated by arrows) but the location of the splitting in  $\mathbf{k}$  space appears to move from band to band as a function of thickness. Although the total number of states crossing  $E_F$  does not vary with Co thickness, the positions of the splittings move monotonically inwards towards  $\mathbf{k}_{\parallel}=0$  about half a band spacing as Co thickness goes from 3 to 8 ML. Beyond 8 ML there is no further evolution of the split states suggesting that the Co states have converged effectively into bulk-like states, at least as far as the overlayer QW states are concerned.

Taken together, Figs. 1–3 demonstrate that the band structure of the Cu/Co/Cu system cannot be regarded as solely a function of the Cu thickness  $d_{\text{Cu}}$  but that the Co thickness  $d_{\text{Co}}$  must be taken into account as well. Because the photoemission technique probes only the outermost 1–3 ML of the sample, it is clear that the QW wave function is significantly modified throughout the layer structure by changes to both thicknesses  $d_{\text{Cu}}$  and  $d_{\text{Co}}$ . Therefore calculations must explicitly take both thicknesses into account to understand the elec-

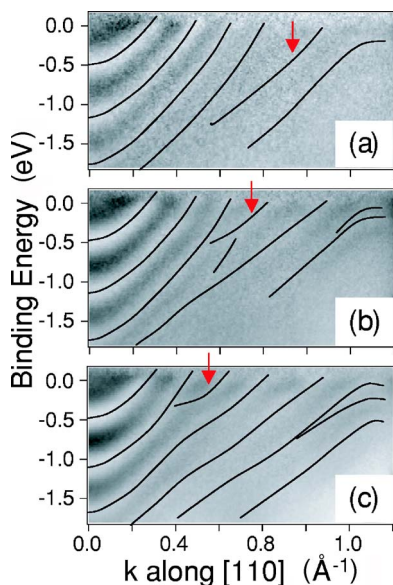


FIG. 3. (Color online) QW dependence on Co barrier thickness. (a–c) Band maps of Cu/Co/Cu(001) with fixed  $d_{\text{Cu}}=19$  ML and nominal  $d_{\text{Co}}=3, 4, 8$  ML, resp. The lines are visual guides for the eye.

tronic properties of our structures and hence the magnetic coupling properties of giant magnetoresistance devices. Unfortunately, self-consistent calculations are difficult owing to the large number of atoms in the unit cell of the layered structure—typically 20 ML Cu+8 ML Co+ $\infty$  substrate Cu atoms. Instead, we can only use a few layers of Cu to represent the effects of the infinitely thick substrate.

Qualitatively speaking, as a Cu QW electron is reflected by the Co layer, it interacts with the Co electronic states with the same energy and the same in-plane momentum. This kind of interaction usually results in a state crossing effect which leads to the QW state evolving into another QW state. From the scattering point of view, the interaction of the Cu electron with the Co state leads to a rapid phase change of the QW states, which moves the QW state from one branch to another. This effect was recently reported in the Ag/Ge(111) system,<sup>4</sup> but a qualitative explanation seems difficult because the photoemission intensity depends on many factors (e.g., polarization direction, x-ray incident angle, final state properties, etc.) in addition to the energy band structure. In an attempt to prove the Co state origin in the anomalous photoemission result, we carried out a first principle calculation for the Cu/Co(100) system.

Calculations were carried out for three-layer systems with thicknesses ( $d_{\text{Cu}}, d_{\text{Co}}, d_s$ ) where  $d_s$  is the finite thickness of a substrate copper slab ( $d_s=\infty$  in the experiment). The calculations were based on density functional theory<sup>8–10</sup> and the Perdew–Burke–Ernzerhof generalized gradient approximation<sup>11,12</sup> to the exchange–correlation functional, as implemented in the norm-conserving pseudopotential plane-wave parallel codes PARATEC and PEtot.<sup>13</sup> Pseudopotentials of the Hammann and Troullier–Martins type<sup>14–16</sup> were generated with the fhi98PP pseudopotential program. The  $3s$ ,  $3p$ , and  $3d$  states are included for the Cu and Co valence electrons. The calculations performed in this paper are identical

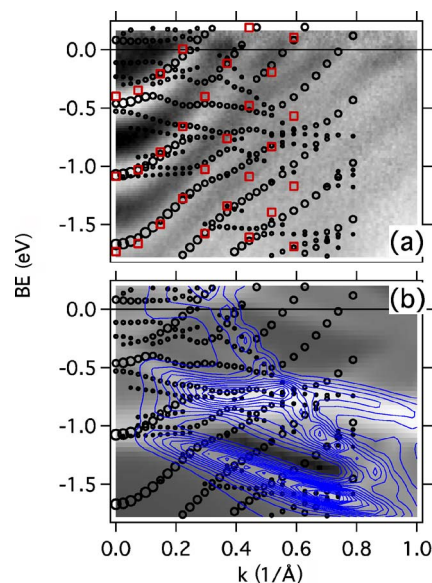


FIG. 4. (Color online) Comparison of calculations and experimental QW states. (a) Experiment for [Cu, Co, Cu(100)] thicknesses (19, 8,  $\infty$ ) (grayscale) vs calculations for isolated QW (19, 0, 0) (squares) and realistic slab model (19, 8, 4) (circles). (b) Comparison of slab calculations (19, 8, 4) to density of states (grayscale, lighter meaning denser) and weighted density of states (contours) of the Co substrate.

to those performed in Ref. 6 with the exception that here we carried out  $\mathbf{k}_{\parallel}$ -dependent calculations while Ref. 6 only contains results at the surface Brillouin zone center,  $\bar{\Gamma}$ .

Figure 4(a) shows a comparison of our experimental results for  $(d_{\text{Cu}}, d_{\text{Co}}, d_s)=(19, 8, \infty)$  ML to the calculated results for a realistic (19, 8, 4) ML system (circles) and for an isolated copper slab, (19, 0, 0) (squares). The size of each circle (which represents one state in our calculation) is scaled according to the percentage of its wave function  $|\phi|^2$  in the surface Cu layer in order to approximate the intensity seen by photoemission. Comparing our calculated results with and without the Co layer, we find that they are similar at  $\mathbf{k}_{\parallel}=0$ , which means the Co layer serves only as a barrier at  $\mathbf{k}_{\parallel}=0$ ; there is little mixing of the Co states with the Cu quantum well states. However, at  $k_{\parallel}>0$ , the calculated (19, 8, 4) ML system has many more states around the energy of  $-0.5$  eV. These extra states indicate the interaction of the Co states with the Cu quantum well states at  $k_{\parallel}>0$ . Interestingly, our calculated states for (19, 0, 0) ML lie on top of the experimental emission intensity bands, including the extra (“split”) band shown with an arrow in Figs. 1 and 3. According to this, these seemingly extra bands are in fact the original Cu quantum well bands, but intercepted in the middle by Co states as shown in Fig. 4(a). These Co mixing states intrude into the original Cu quantum well bands, break them up, and make them appear like band splitting.

Our calculated states for the (19, 8, 4) ML system [Fig. 4(a)] are more complicated than the experiment, having more intrusion states than in the experimental data. This may follow from the finite total slab thickness imposed by our calculation—states which would leak away into the infinite substrate if our  $d_s=\infty$  appear in our simulations of  $d_s=4$  with

significant surface weight. It may also be due to energy broadening in the experiment, such as smearing resulting from layer thickness inhomogeneities.

In order to better understand the interaction of the Co and Cu QW states at  $k_{\parallel} > 0$  we follow Aballe *et al.*<sup>2</sup> and plot the density of states (DOS) of the bulk Co, integrated along  $k_{[001]}$ , as a grayscale on top of the calculated Cu QW states in Fig. 4(b). The Co DOS in this binding energy range is dominated by minority  $d$  states.

We have also calculated a weighted DOS related to possible coupling between the Co  $d$  states and the Cu QW states by adding a coupling strength factor  $|\int_A \psi'_{\text{Co}}(k_{[110]}, k_{[001]}) \psi'_{\text{Cu}}(k_{[110]}, k'_{[001]}) dx dy|^2$  to each Co state  $\psi_{\text{Co}}(k_{[110]}, k_{[001]})$ ; this factor is used as a weight for each band structure point  $E_{\text{Co}}(k_{[110]}, k_{[001]})$ . Here the Cu state  $k'_{[001]}$  is chosen so that the Cu state  $\psi_{\text{Cu}}(k_{[110]}, k'_{[001]})$  has roughly the same energy as the corresponding Co state  $\psi_{\text{Co}}(k_{[110]}, k_{[001]})$ . The  $\psi'$  indicates the  $z$  derivative of the wave function, and the area integral  $dx dy$  is done on the (001) interface between the Co and Cu layers. The resulting weighted DOS is plotted as contours in Fig. 4(b). A similar weight factor using  $\psi_{\text{Co}}, \psi_{\text{Cu}}$  instead of  $\psi'_{\text{Co}}, \psi'_{\text{Cu}}$  has also been calculated. The result is somewhat similar, but we found that the present weighted DOS is more satisfactory.

We see that the Co DOS, especially the weighted DOS, coincides with the directly calculated intrusion states. This confirms our assumption that these intrusion states come from the mixing of the Co minority  $d$  states with Cu QW states. A more subtle effect shows up at the bottom of the Fig. 4(b). There is a slight kink in the directly calculated band, which coincides with the second dominant peak in the weighted DOS. The same kink might also exist in the experimental data, although it is too subtle to be positively confirmed there.

Recently, similar effects were reported for the band structure of 8–9 ML Ag on Ge(111).<sup>4</sup> There the substrate bands

were treated as a continuum interacting with discrete QW states, leading to a change in the self-energy of the quasiparticles as they cross the substrate band edge. It is not clear that this approach could qualitatively explain our data, because we do not observe an increase in linewidth of the QW states in the Co band interaction region as required by causality.<sup>17</sup> Furthermore, the Co  $d$  state band dispersions are more complicated than the simple  $sp$  Ge bands and lead to a more complicated splitting behavior. Our approach, while tentative due to the computational burden, can at least qualitatively explain the apparent “splitting” and could be used as a predictive tool for wave function engineering.

In summary, we have experimentally found and theoretically confirmed a dramatic modification to the band structure of Cu thin films on Co/Cu(001) induced by the Co barrier layer’s electronic structure. Since the barrier layer’s electronic properties can be chosen at will, in principle the singular behavior of the bands (at present mostly near 0.4 eV below  $E_F$ ) could be moved to the Fermi level. This would make the electronic response function of the quantum wells exquisitely sensitive to changes in the barrier layer’s band structure, leading to control of the coupling behavior of magnetic multilayer devices.

This research used resources of the National Energy Research Scientific Computing Center and the Advanced Light Source, which are supported by the Office of Science of the U.S. Department of Energy. The Advanced Light Source is supported by the Director, Office of Science, Office of Basic Energy Sciences, Materials Sciences Division, of the U.S. Department of Energy under Contract No. DE-AC03-76SF00098 at Lawrence Berkeley National Laboratory. This experimental work was funded in part by the National Science Foundation under Contract No. DMR-0110034. The theoretical work was supported in part by the Laboratory Directed Research and Development Program of Lawrence Berkeley National Laboratory under the Department of Energy Contract No. DE-AC03-76SF00098.

<sup>1</sup>N. V. Smith, N. B. Brookes, Y. Chang, and P. D. Johnson, *Phys. Rev. B* **49**, 332 (1994), and references therein.

<sup>2</sup>L. Aballe, C. Rogero, P. Kratzer, S. Gokhale, and K. Horn, *Phys. Rev. Lett.* **87**, 156801 (2001).

<sup>3</sup>F. G. Curti, A. Danese, and R. A. Bartynski, *Phys. Rev. Lett.* **80**, 2213 (1998).

<sup>4</sup>S.-J. Tang, L. Basile, T. Miller, and T.-C. Chiang, *Phys. Rev. Lett.* **93**, 216804 (2004).

<sup>5</sup>R. K. Kawakami, E. Rotenberg, E. J. Escorcia-Aparicio, H. J. Choi, T. R. Cummins, J. G. Tobin, N. V. Smith, and Z. Q. Qiu, *Phys. Rev. Lett.* **80**, 1754 (1998).

<sup>6</sup>J. M. An, D. Raczkowski, Y. Z. Wu, C. Y. Won, L. W. Wang, A. Canning, M. A. VanHove, E. Rotenberg, and Z. Q. Qiu, *Phys. Rev. B* **68**, 045419 (2003).

<sup>7</sup>W. L. Ling, E. Rotenberg, H. J. Choi, J. H. Wolfe, F. Toyama, S. Paik, N. V. Smith, and Z. Q. Qiu, *Phys. Rev. B* **65**, 113406 (2002).

<sup>8</sup>P. Hohenberg and W. Kohn, *Phys. Rev.* **136**, B864 (1964).

<sup>9</sup>W. Kohn and L. J. Sham, *Phys. Rev.* **140**, 1133 (1965).

<sup>10</sup>J. von Barth and L. Hedin, *J. Phys. C* **5**, 1629 (1972).

<sup>11</sup>J. P. Perdew, J. A. Chevary, S. H. Vosko, K. A. Jackson, M. R. Pederson, D. J. Singh, and C. Fiolhais, *Phys. Rev. B* **46**, 6671 (1992).

<sup>12</sup>J. P. Perdew, K. Burke, and M. Ernzerhof, *Phys. Rev. Lett.* **77**, 3865 (1996).

<sup>13</sup>The plane-wave pseudopotential code PETot was originally developed by L. W. Wang while at the National Renewable Energy Laboratory; PARATEC (Parallel Total Energy Code) by B. Pfrommer, D. Raczkowski, A. Canning, and S. G. Louie, Lawrence Berkeley National Laboratory with contributions from F. Mauri, M. Cote, Y. Yoon, C. Pickard, and P. Haynes.

<sup>14</sup>M. Fuchs and M. Scheffler, *Comput. Phys. Commun.* **119**, 67 (1999).

<sup>15</sup>D. R. Hamann, *Phys. Rev. B* **40**, 2980 (1989).

<sup>16</sup>N. Troullier and J. L. Martins, *Phys. Rev. B* **43**, 1993 (1991).

<sup>17</sup>T. Valla, A. V. Fedorov, P. D. Johnson, and S. L. Hulbert, *Phys. Rev. Lett.* **83**, 2085 (1999).